Available online at www.sciencedirect.com
ScienceDirect
Journal of Power Sources 168 (2007) 66–78
JOURNAL OF POWER SOURCES
www.elsevier.com/locate/jpowsour

Model prediction for ranking lead-acid batteries according to expected lifetime in renewable energy systems and autonomous power-supply systems

Julia Schiffer [a,*], Dirk Uwe Sauer [a], Henrik Bindner [b], Tom Cronin [b], Per Lundsager [b], Rudi Kaiser [c]

[a] *RWTH Aachen University, Electrochemical Energy Conversion and Storage Systems Group, Jägerstrasse 17/19, D-52066 Aachen, Germany*
[b] *RISOE National Laboratory, Roskilde, Denmark*
[c] *Fraunhofer Institute for Solar Energy Systems ISE, Freiburg, Germany*

Received 23 September 2006; accepted 28 November 2006
Available online 20 December 2006

Paper presented at 10th ELBC

Abstract

Predicting the lifetime of lead-acid batteries in applications with irregular operating conditions such as partial state-of-charge cycling, varying depth-of-discharge and different times between full charging is known as a difficult task. Experimental investigations in the laboratory are difficult because each application has its own specific operation profile. Therefore, an experimental investigation is necessary for each application and, moreover, for each operation strategy.

This paper presents a lifetime model that allows comparison of the impact of different operating conditions, different system sizing and different battery technologies on battery lifetime. It is a tool for system designers and system operators to select appropriate batteries, to do a proper system design (sizing of the battery, power generators and loads), and to implement an optimized operation strategy (end-of-charge voltage, frequency of full charging, gassing periods, maximum depth-of-discharge).

The model is a weighted Ah throughput approach based on the assumption that operating conditions are typically more severe than those used in standard tests of cycling and float lifetime. The wear depends on the depth-of-discharge, the current rate, the existing acid stratification, and the time since the last full charging. The actual Ah throughput is continuously multiplied by a weight factor that represents the actual operating conditions.

Even though the modelling approach is mainly heuristic, all of the effects that are taken into account are based on a detailed analysis and understanding of ageing processes in lead-acid batteries. The 'normal' user can adapt the model to different battery types simply from the data sheet information on cycle lifetime and float lifetime.

Keywords: Lead-acid battery; Ageing; Lifetime model; Photovoltaic; Wind

1. Introduction

Predicting the lifetime of lead-acid batteries in renewable energy systems or autonomous power supply systems without extended laboratory tests is very difficult. This is mainly due to the fact that the cycling regime is very irregular, full chargings are rare, charging and discharging are intercepting each other frequently, and a wide range of charge and discharge currents occurs.

A combined performance and lifetime model has been formulated. The lifetime part of the model is developed to predict the lifetime of batteries under such operating conditions for use in system design tools. Adaptation of the model to different battery products is solely based on the lifetime data given by the manufacturers for regular cycling (cycle lifetime) and for float

* Corresponding author. Tel.: +49 241 80 96935; fax: +49 241 80 92203.
E-mail addresses: batteries@isea.rwth-aachen.de, sf@isea.rwth-aachen.de (J. Schiffer).

0378-7753/$ – see front matter © 2006 Elsevier B.V. All rights reserved.
doi:10.1016/j.jpowsour.2006.11.092

operation (float lifetime). From these data, the expected lifetime under irregular cycling conditions is calculated. The model is based on the concept of 'weighted Ah throughput'. For a regular full cycle, the weighting factor is 1. By contrast, severe operating conditions – defined through partial state-of-charge cycling, cycling with significant acid stratification, high temperature and time since the last full charging – are weighted with factors larger than 1. A battery has reached the end of its lifetime if the weighted Ah throughput is equivalent to the Ah throughput achievable with regular cycling (cycle lifetime). Corrosion effects are calculated based on battery voltage and temperature taking into account the float lifetime defined by the manufacturer.

In summary, different operating profiles (depending on system sizing and operation strategy) can be analyzed with regard to their impact on battery lifetime. System designers can use the model to select the appropriate battery brand, battery technology and battery size for a certain application. The concept of the model, its application in system design tools, and verification against measured data is presented.

2. Physico-chemical processes

Even though the model presented in this paper does not constitute a physico-chemical approach, all concepts and the theoretical background for different parts of the model are based on physical and chemical processes that occur in lead-acid batteries. The basic assumptions underlying the model are described briefly in this section. This list does not aim to be a complete description of all processes that occur in lead-acid batteries. Furthermore, the authors are aware of the fact that while different processes are described and modelled in a simplified way, other processes are discussed controversially within the scientific community. Each part of the model is based on a certain assumption that shows its ability to represent the impact of certain operating conditions on the battery lifetime.

Grid corrosion of the positive electrode and degradation of the active material are the two ageing mechanisms that are considered in the model. Acid stratification, gassing and the structure of the lead sulfate crystals are taken into account because of their direct impact on battery ageing.

2.1. Corrosion

Corrosion means a conversion of the lead grid of the positive electrode into different lead oxides that form a layer with a complex structure on the grid. This leads to lower conductivity of the grid because of its reduced diameter and the increase in resistance across the corrosion layer between the grid and the active material. The corrosion products have a lower density and therefore a higher specific volume. This results in mechanical stress and therefore in a loss of active material because parts of the corrosion layer flake off and thus interrupt the contact between the grid and the active material. The modelling approach is based on the measurements and the theoretical concepts of the corrosion process in lead-acid batteries that have been presented by Lander [1–3] and Ruetschi et al. [4–6] some 40–50 years ago. Corrosion of the negative electrode, that has been described by different authors mainly for VRLA batteries (e.g., [7]), is not taken into account in this model.

2.2. Acid stratification

Acid stratification itself is not an ageing effect, but it accelerates ageing. It is fully reversible at any time if sufficient gas evolves or if electrolyte agitation systems are used. Acid stratification builds up during charging and discharging and results in a gradient of the acid concentration. Diffusion and gassing bring a mixing of the electrolyte.

Ageing as a result of acid stratification occurs because the differences in the acid concentration result in different electrochemical potentials at different levels in the battery. Therefore, the current distribution along the electrodes is inhomogeneous. Charging is preferred in the upper parts of the electrode (lower density, lower potential), discharging is preferred in the lower part of the electrode (higher density, higher potential). Consequently, the state-of-charge in the lower part of the electrode is significantly lower compared with the upper part and therefore sulfation is accelerated. This has been confirmed by models [8] and measurements [9]. Post-mortem analysis of lead-acid batteries in cyclic operation with insufficient regular full charging shows a very high degree of irreversible sulfation in the lower part of the electrodes [10,11].

The impact of acid stratification on ageing depends on the existing gradient in acid concentration. This can be modelled in detail with a finite difference or finite element analysis. Nevertheless, this is far beyond of the scope of the model proposed here. Therefore, an increase in acid stratification with Ah throughput as well as minimum state-of-charge since the last full charge and a mixing through diffusion and gassing is assumed. The maximum acid stratification is limited and ageing depends mainly on the assumption that it is accelerated by the low state-of-charge of the lower part of the electrode. When VRLA batteries or flooded batteries with an electrolyte agitation system are used, no acid stratification is assumed and therefore there is no contribution to battery ageing.

2.3. Gassing

Gassing is by far the most important side-reaction in lead-acid batteries. It occurs when the cell voltage is so high that hydrogen evolves at the negative electrode and oxygen at the positive electrode. The gassing current increases with increasing cell voltage according to a Butler-Volmer process, and with increasing battery temperature according to the Arrhenius law. Gassing reduces the coulombic efficiency and results in mixing of the electrolyte in flooded batteries.

2.4. Sulfation and sulfate crystal growth

Lead sulfate ($PbSO_4$) is created during discharging at both the positive and the negative electrode. During charging, the crystals are converted back to the respective active material. Crystals that cannot be removed during standard charging cannot

contribute any longer to the capacity of the battery. This effect is called 'sulfation'. As a basis for the model, the process of Pb^{2+} dissolution in the electrolyte during discharging and the subsequent nucleation as sulfate crystals is assumed as the reaction mechanism.

In addition to the fact that some material no longer takes part in the cycling process, the size of the crystals is of relevance to the electrical performance of the battery. The smaller the crystals, the larger is the overall surface of the crystals, assuming a constant crystal volume for the sum of all crystals. The dissolution of the sulfate crystals, which is necessary during the charging process, is directly proportional to the crystal surface. The lower the crystal surface, the higher is the overvoltage during charging. Therefore, batteries with large sulfate crystals will reach the maximum charging voltage earlier than those with small crystals. As a result, the overall charging process takes longer for the battery with the large crystals. In solar applications, the charging time is limited by the available sunshine hours. Therefore, a battery with larger crystals will reach a full charging more rarely than a battery with small crystals. Experimental evidence for the described process has been obtained in a previous study [12].

The following model can be used to estimate the number of crystals and therefore their size. Assuming that the battery is fully charged at the beginning of a discharge and that there are no lead sulfate residues, there are no seed crystals on which the $PbSO_4$ molecules can accumulate. New crystals are formed only when the ion concentration becomes very high compared with the saturation concentration. A high ion concentration results in a high overvoltage and therefore a significant voltage dip at the beginning of a discharge process can be observed after complete full charging; this is also known as the 'Spannungssack' or 'coup de fouet'. In the following discharge, no more crystals are formed because the ion concentration never becomes high enough again. As a consequence, new crystals are only created at the beginning of a discharge. The smaller the current is at the beginning of the discharge the smaller is the number of crystals that are created because there are less Pb^{2+} ions and the crystals have more time to grow. In succession, at the same depth-of-discharge, the crystals will be larger with a small current at the beginning of the discharge than with a higher current. The process has been described mathematically by Kappus [13] and has been included in a full battery model in Ref. [8]. Recently, different authors reported that the above-described mechanism might be an incorrect interpretation of the measured data [14,15]. As, however, the above described mechanism describes very well the experimentally observed results, we keep this as the basis for our model.

2.5. Degradation of active material

Degradation is a general term for processes that result in a capacity loss due to changes in the active mass structure and composition. Major contributions to degradation come from loss of active material due to shedding (mechanical loosening due to gassing and active mass expansion–contraction), sulfation (irreversible lead sulfate crystals) and softening (loosening of the particles of the active mass resulting in a loss of electronic conductivity).

The mechanical stress is caused either by gassing or by 'breathing' of the active mass. 'Breathing' is caused by a difference in the specific volume of lead sulfate (discharged material) and that of lead (negative electrode, volume change factor 2.4) or lead dioxide (positive electrode, volume change factor 1.96) in the charged materials. This is the major reason why the cycle lifetime of lead-acid batteries depends strongly on the depth-of-discharge during cycling. The lower the state-of-charge, the higher is the mechanical stress.

3. Description of model

A simplified flow diagram of the model is given in Fig. 1. During one simulation step, the voltage and the state-of-charge (SoC) are determined on the basis of the battery parameters. The voltage is calculated according to a modified Shepherd equation [8,16,17]. The SoC is calculated by integrating the difference between the total battery current and the gassing current. Based on voltage and SoC, corrosion and degradation parameters are determined and then used to change the battery parameters and to determine the remaining capacity of the battery, which is the main output of the model. 'Remaining capacity' signifies the capacity of the battery in its fully-charged state for a defined discharge current rate (typically the 10 h current).

Many calculations are also influenced by the battery temperature, which is determined from the ambient temperature conditions. Different scenarios can be chosen, where the battery temperature is equal to either the ambient temperature at all times (simplest approach) or an average of the ambient temperature over a certain duration (simulating indoor conditions). These approaches work well for all applications with average currents below the 10 h rate, because the heating-up of the battery due to the operating current can be neglected. For applications with higher average currents, the integration of a full battery temperature simulation model is possible without major problems, if required (e.g., [18]).

The functions, which are used to represent the different effects, are in fact in parts of heuristic nature. They are always based on the knowledge of real physical or chemical processes

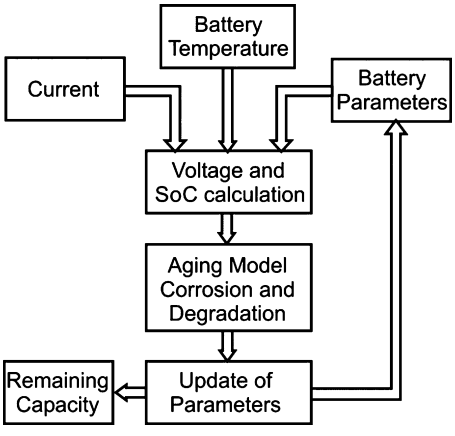

Fig. 1. Simplified flow diagram of model.

as described above, but as this models aims at being a simple computing approach, generalized approaches must be used. Nevertheless, it is not possible to explain in each case why, for example, a function such as $\sqrt{X}$ is used instead of e.g., $\sqrt[3]{X}$. The choice has been made according to expert knowledge and comparison of measured data with model calculations.

3.1. Current–voltage characteristics

To be able to calculate the different ageing mechanisms, the existing state of the battery has to be known, which is mainly the voltage of the cell. The voltage is decisive for corrosion and SoC, which also needs the gassing current as an input. The calculation of these values is given in this section.

The cell voltage is calculated according to a modified Shepherd equation (Eq. (1)). It consists of four terms. The first is the open-circuit voltage at full-charge. The second term is associated with the change in open-circuit voltage with SoC. The third term describes the ohmic losses, represented by an ohmic resistance. Major contributors are the grid resistance, the active mass resistance, and the resistance of the electrolyte. The fourth term models the overvoltage as a function of current and SoC and contributes most when the battery is close to full charge or full discharge. No dynamic terms are included because the model is developed for time-step evaluations with time-steps not less than 1 min. Therefore, transient effects with short time constants are not considered. Anyhow, the transient effects have no known effect on the battery lifetime. Different sets of parameters are used for charging and discharging, namely:

$$U(t)=U_0 - g\,\mathrm{DoD}(t) + \rho_\mathrm{c}(t)\frac{I(t)}{C_\mathrm{N}} + \rho_\mathrm{c}(t)M_\mathrm{c}\frac{I(t)}{C_\mathrm{N}}\frac{\mathrm{SoC}(t)}{C_\mathrm{c}-\mathrm{SoC}(t)}, \quad \forall I(t) > 0,$$

$$U(t) = U_0 - g\,\mathrm{DoD}(t) + \rho_\mathrm{d}(t)\frac{I(t)}{C_\mathrm{N}} + \rho_\mathrm{d}(t)M_\mathrm{d}\frac{I(t)}{C_\mathrm{N}}\frac{\mathrm{DoD}(t)}{C_\mathrm{d}(t)-\mathrm{DoD}(t)}, \quad \forall I(t) \le 0 \tag{1}$$

where: U [V] is the terminal voltage of the cell; U_0 [V] is the open-circuit equilibrium cell voltage at the fully-charged state (Eq. (2)); g [V] is an electrolyte proportionality constant (Eq. (3)); SoC is the state-of-charge (SoC = 1 for a fully-charged battery, SoC = 0 after discharge of the nominal capacity, SoC < 0 is possible); DoD = 1 − SoC is the depth-of-discharge; $\rho_\mathrm{c}/\rho_\mathrm{d}$ [Ω Ah] is the aggregated internal resistance; I [A] is the applied current (charge: $I > 0$; discharge: $I \le 0$); C_N [Ah] is the nominal capacity; $M_\mathrm{c}/M_\mathrm{d}$ is the charge-transfer overvoltage coefficient; $C_\mathrm{c}/C_\mathrm{d}$ is the normalized capacity. The index 'c' indicates charging and the index 'd' indicates discharging.

Although the Shepherd equation is developed for discharge conditions [16], it is assumed that the structure is the same for charge conditions, but with a different set of parameters [17,19]. The parameters can be found through parameter identification from measured data. In the original Shepherd-based model, it was assumed that all the model parameters are constant, both over time and independent of operating conditions. Here, the two resistance coefficients ρ_c and ρ_d as well as the discharge capacity C_d change according to the different ageing mechanisms.

The extension of the Shepherd model to charging was undertaken in Refs. [17,19] by using a completely separate set of parameters for charging and discharging that included the parameters U_0 and g. Because of the additional degrees of freedom with the additional parameters, it is easier to adapt the model to measured data. Nevertheless, different parameters for calculating the open-circuit voltage (OCV) as a function of the SoC also results in discontinuities when changing between charging and discharging. Furthermore, the OCV is directly coupled to the acid concentration and is directly proportional to the SoC, given that there is no acid stratification. The parameters U_0 and g can be calculated directly from the data sheet information on the nominal acid concentration (ρ_nominal), the weight (m) of the acid in the cell, and the nominal capacity of the battery cell (C_nominal). All data are given for a single cell. For the calculation of the OCV (U_0) of the fully-charged battery, the rule-of-thumb is chosen as given in Eq. (2). The offset parameter reported in the literature is typically 0.84–0.86 V. For the model, 0.86 V is chosen due to the fact that, on average, a certain acid stratification can be assumed and therefore the OCV is above the value for a battery with a homogenous electrolyte:

$$U_0 = 0.86\,\mathrm{V} + 1\,\mathrm{V\,g^{-1}\,cm^3}\cdot\rho_\mathrm{nominal} \tag{2}$$

$$g = 1\,\mathrm{V\,g^{-1}\,cm^3}\cdot(\rho_\mathrm{nominal} - \rho_\mathrm{empty}) \tag{3}$$

$$\rho_\mathrm{empty} = a_\rho + \sqrt{b_\rho + \frac{c_\rho\rho_\mathrm{nominal}}{m}((d_\rho + e_\rho\rho_\mathrm{nominal})m - f_\rho C_\mathrm{nominal})} \tag{4}$$

where $a_\rho = 0.4956\,\mathrm{g\,cm^{-3}}$, $b_\rho = 0.2456\,\mathrm{g^2\,cm^{-6}}$, $c_\rho = 77.53\,\mathrm{cm^3}$, $d_\rho = -0.01278\,\mathrm{g\,cm^{-6}}$, $e_\rho = 0.01289\,\mathrm{cm^{-3}}$, and $f_\rho = 0.0373\,\mathrm{g^2\,Ah^{-1}\,cm^{-6}}$.

Eq. (4) for the calculation of ρ_empty is based on the relation of acid density and acid concentration taking into account the use of sulfuric acid. The data are taken from Ref. [7].

Corrosion mostly affects the positive electrode. Therefore, only the voltage of the positive electrode is considered for corrosion calculation using a modified Shepherd equation that provides just the voltage of the positive electrode:

$$U_\mathrm{corr}(t) = U_\mathrm{corr,0} - \frac{10}{13}g\,\mathrm{DoD}(t) + 0.5\rho_\mathrm{c}(t)\frac{I(t)}{C_\mathrm{N}} + 0.5\rho_\mathrm{c}(t)M_\mathrm{c}\frac{I(t)}{C_\mathrm{N}}\frac{\mathrm{SoC}(t)}{C_\mathrm{c}-\mathrm{SoC}(t)}, \quad \forall I > 0,$$

$$U_\mathrm{corr}(t) = U_\mathrm{corr,0} - \frac{10}{13}g\,\mathrm{DoD}(t) + 0.5\rho_\mathrm{d}(t)\frac{I(t)}{C_\mathrm{N}} + 0.5\rho_\mathrm{d}(t)M_\mathrm{d}\frac{I(t)}{C_\mathrm{N}}\frac{\mathrm{DoD}(t)}{C_\mathrm{d}(t)-\mathrm{DoD}(t)}, \quad \forall I \le 0 \tag{5}$$

with the corrosion voltage of the fully-charged battery without current flow $U_\mathrm{corr,0}$, which is a function of the acid concentration (e.g., 1.75 V for an acid concentration of 30% [7]).

The contribution of ohmic losses and the charge factor are assumed to be equally distributed between the positive and the negative electrode. The factor 10/13 for the SoC influence was derived as follows: a typical change in the OCV from fully charged to fully discharged is 130 mV. Approximately 100 mV of this change can be attributed to the positive electrode and 30 mV to the negative electrode [7,8].

3.2. Gassing current and state of-charge

The gassing reaction shows a Butler-Volmer characteristic. Due to the high overpotentials, however, the Tafel approximation can be employed [20]. Quantitatively, the gassing current can be calculated from the following equation, which is derived from the Tafel approximation:

$$I_{\text{gas}} = \frac{C_{\text{N}}}{100\,\text{Ah}} I_{\text{gas},0}\, \exp(c_{\text{u}}(U - U_{\text{gas},0}) + c_{\text{T}}(T - T_{\text{gas},0})) \tag{6}$$

where: $I_{\text{gas},0}$ is the normalized gassing current for a 100 Ah nominal battery capacity at nominal voltage $U_{\text{gas},0}$ and nominal temperature $T_{\text{gas},0}$; c_{u} is the voltage coefficient; c_{T} is the temperature coefficient; U is the cell voltage; T is the battery temperature. With this approach, most parameters remain unchanged during the lifetime of the battery except for the normalized gassing current which increases with ageing ($I_{\text{gas},0}(t)$). For flooded batteries, enhanced gassing can be easily explained by increasing antimony deposition on the negative electrode. The antimony is released from the positive grid as a result of the corrosion process. This reduces the hydrogen overpotential and hence enhances the gassing rate. It is assumed that the gassing current increases proportionally to the increase in internal resistance. This relation is also a good approximation for valve-regulated (VRLA) batteries. The internal resistance of such batteries increases mainly due to loss of water and therefore reduced conductivity of the electrolyte. But while water is lost, the pores are increasing and therefore gas transport from one electrode to the other is improved and finally results in increased gassing that is represented by an increase in the normalized gassing current.

The SoC is calculated by integrating the current minus the gassing current divided by the nominal capacity, i.e.:

$$\text{SoC}(t) = \text{SoC}(0) + \int_0^t \frac{I(\tau) - I_{\text{gas}}(\tau)}{C_{\text{N}}}\,\text{d}\tau \tag{7}$$

A SoC of 1 always represents the state where sulfate crystals that can contribute to the charge/discharge capacity have been converted completely into PbO_2 or Pb as the positive or negative electrode, respectively.

3.3. Corrosion of positive grid

The corrosion model uses the concept of a corrosion 'layer' with lower conductivity, which grows over the lifetime of the battery. Its resistance is added to the resistance of the new battery. An effective layer thickness, ΔW, is correlated with the loss of active material that is assumed to have lost contact. The effective corrosion layer thickness is calculated in each simulation step depending on the corrosion voltage U_{corr} ([8], cf., Section 3.1). The corrosion processes and products vary according to the potential. Therefore, different descriptions of the corrosion layer growth have been used according to Lander [1–3]:

$$\begin{aligned} &(U_{\text{corr}} < 1.74) \quad \Delta W(t) = k_{\text{s}} x^{0.6} \quad \text{where } x = \left(\frac{\Delta W(t-\Delta t)}{k_{\text{s}}}\right)^{1/0.6} + \Delta t \\ &(U_{\text{corr}} \geq 1.74) \quad \Delta W(t) = \Delta W(t-\Delta t) + k_{\text{s}}\,\Delta t \end{aligned} \tag{8}$$

where Δt is the duration of one time step and k_{s} is the corrosion speed parameter, which signifies the increase in the corrosion layer with time. The parameter k_{s} is calculated according to Arrhenius' law:

$$k_{\text{s}}(U_{\text{corr}}, T) = k(U_{\text{corr}})\, \exp(k_{\text{s,T}}(T - T_{\text{corr},0})) \tag{9}$$

where $k(U_{\text{corr}})$ is a corrosion speed/voltage curve based on the work of Lander [3]. The temperature factor $k_{\text{s,T}} = \ln(2)/15\,\text{K}$ reflects the fact that the corrosion speed doubles for a temperature increase of 15 K or slows down at low temperatures. $T_{\text{corr},0} = 298\,\text{K}$ is a reference temperature.

The resistance ρ_{corr} of the corrosion layer and the capacity loss C_{corr} both depend on the corrosion layer thickness ΔW, i.e.:

$$\begin{aligned} \rho_{\text{corr}}(t) &= \rho_{\text{corr,limit}} \frac{\Delta W(t)}{\Delta W_{\text{limit}}}, \\ C_{\text{corr}}(t) &= C_{\text{corr,limit}} \frac{\Delta W(t)}{\Delta W_{\text{limit}}} \end{aligned} \tag{10}$$

All parameters with the index 'limit' are the corresponding values that result from keeping the battery on float charge until the end of life (float lifetime). The calculation of $\rho_{\text{corr,limit}}$ and $C_{\text{corr,limit}}$ is based on the assumption that 20% of the capacity decrease at the end of life is caused by an increase in the internal resistance from corrosion, and that the remaining 80% of the capacity decreases due to the loss of active material from corrosion. This relation has been proposed by Stöcklein [19] and successfully used by Puls [21] and Sauer [8]. ΔW_{limit} is defined as the corrosion layer thickness when the battery has reached its end of life, which is at the end of the float lifetime L given in the data sheet. To calculate ΔW_{limit}, the float lifetime is multiplied by the corrosion speed parameter $k_{\text{s,limit}}$ taken from the curve $k(U_{\text{corr}})$ at the voltage $U_{\text{corr}} = U_{\text{float}}$, i.e.:

$$\Delta W_{\text{limit}} = L k_{\text{s,limit}} \tag{11}$$

3.4. Degradation of active mass

Degradation represents the capacity loss caused by cycling of the battery. The IEC cycling lifetime is typically given in a datasheet and is related to the stage at which the battery is

considered to have a remaining capacity of 80% compared with the nominal capacity. Since ageing results from a combination of cycling and corrosion, the effective number of cycles without corrosion would be higher and, according to Ref. [19], amounts to about 1.6 times the IEC cycle lifetime. The number of nominal cycles, Z_N, is calculated by dividing the discharged Ah by the nominal capacity of the battery, namely:

$$Z_N = \int_0^t \frac{|I_{dch}(\tau)|}{C_N}\,d\tau \tag{12}$$

For calculation of the capacity loss due to degradation, the Ah throughput is weighted with the impact of the SoC, the discharge current and the acid stratification. The weighted number of cycles Z_W is calculated with:

$$Z_W(t) = \frac{1}{C_N}\int_0^t |I_{dch}(\tau)|\, f_{SOC}(\tau)\, f_{Acid}(\tau)\,d\tau \tag{13}$$

where f_{SoC} is a factor for the influence of the SoC, which also includes the impact of the current rate, and f_{Acid} is a factor that represents the impact of acid stratification. Eq. (13) is the core of the modelling approach. The Ah throughput is not only integrated but multiplied with factors that represent the additional stress that occurs due to the actual operating conditions compared with the standard cycling regime used to determine the nominal cycle lifetime. The different weighting factors are described in the following sections.

The capacity loss due to degradation C_{deg} is then:

$$C_{deg}(t) = C_{deg,limit}\, e^{-c_Z(1-(Z_W(t)/1.6Z_{IEC}))} \tag{14}$$

$C_{deg,limit}$ is the capacity at the end of lifetime (i.e., 80%). The parameter c_Z is equal to 5.[1]

3.4.1. Impact of state-of-charge

Degradation increases with decreasing SoC of the battery. The lower the lowest SoC, since the last full charge and the longer the battery remains at a low SoC, the higher is the impact on the battery lifetime. There is a loss of capacity that, on the one hand, arises from the mechanical stress on the active masses due to the DoD and, on the other hand, from the increasing size of the sulfate crystals. These relationships are modelled by the factor f_{SoC}, which is set to 1 at each full charge and which increases with the time since the last full charge, i.e., $\Delta t_{SoC} = t - t_0$, where t_0 is the time of the last full charge and SoC_{min} is the lowest state of charge since the last full charge:

$$f_{SoC}(t) = 1 + (c_{SoC,0} + c_{SoC,min}(1 - SoC_{min}(t)|_{t_0}^{t})) \times f_I(I,n)\,\Delta t_{SoC}(t) \tag{15}$$

The parameters $c_{SoC,0}$ and $c_{SoC,min}$ represent the increase in f_{SoC} with time at SoC = 0 and the influence of SoC_{min}, $f_I(I, n)$ is the current factor, which describes the influence of the current (cf., Section 3.4.2, Eq. (17)).

[1] With the choice of $c_Z = 5$, C_{deg} is not exactly 0 if $Z_W = 0$, but very close. The form of this equation is a compromise to fulfill other boundary conditions: (1) C_{deg} should increase with increasing Z_W; (2) if $Z_W > Z$, $C_{deg} > C_{deg,limit}$.

3.4.2. Impact of sulfate-crystal structure

As mentioned in Section 2.4, small discharge currents result in a lower number but larger lead sulfate crystals compared with those formed at higher discharge rates. The smaller the crystals (with the same volume of lead sulfate), the larger is the surface. Since a large surface makes dissolving of the crystals easier recharging is faster and occurs at lower overvoltages with a fine crystal structure. Accordingly, in applications with limited charging times and limited charging voltage the charging cannot be completed if the sulfate crystals are large. Hence, lead sulfate crystals remain in the electrodes and tend to grow with each cycle. From a certain size onwards, these crystals become inactive. Therefore, there is a clear relationship between current rates and ageing.

The dependence of z on the discharge current I can be derived from data in Ref. [8]. The calculation of the data in Ref. [8] is based on a model presented in Ref. [13]. Numerical fits give the best results with a function of the following type:

$$z = z_0\left(\frac{I}{C_N}\right)^{1.5} \tag{16}$$

where $z_0 = 2.961 \times 10^{11}\ cm^{-3}$. A plot of this function is given in Fig. 2.

Since the number of crystals only changes at the beginning of a discharge, it does not change with the DoD, therefore z is independent of DoD. The influence of the current is related to the surface of the lead sulfate crystal, i.e.:

$$f_I(I) = \frac{A_{ref}}{A(I)} = \frac{r_{ref}^2 z_{ref}}{r^2(I) z(I)} = \left(\sqrt[3]{\frac{z(I)}{z_{ref}}}\right)^2 \frac{z_{ref}}{z(I)} = \sqrt[3]{\frac{z_{ref}}{z(I)}} = \sqrt{\frac{I_{ref}}{I}} \tag{17}$$

All variables marked with the index 'ref' are calculated for a reference current I_{ref} (typically the 10 h current). For higher current rates, the lifetime increases, whereas lower currents decrease the cycle lifetime.

Since the number of crystals is mainly influenced by the discharge current at the beginning of a discharge starting from a fully-charged battery, this current is used for the calculation of

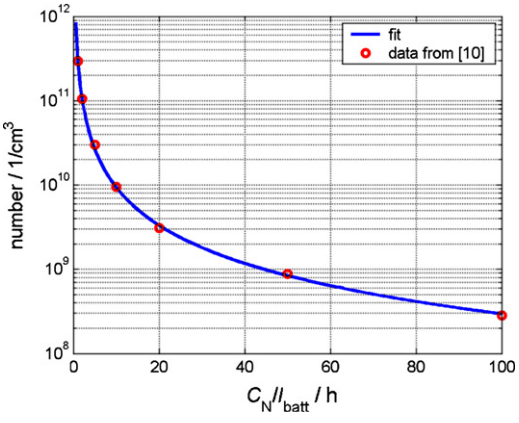

Fig. 2. Number of crystals as a function of discharge current (25 °C).

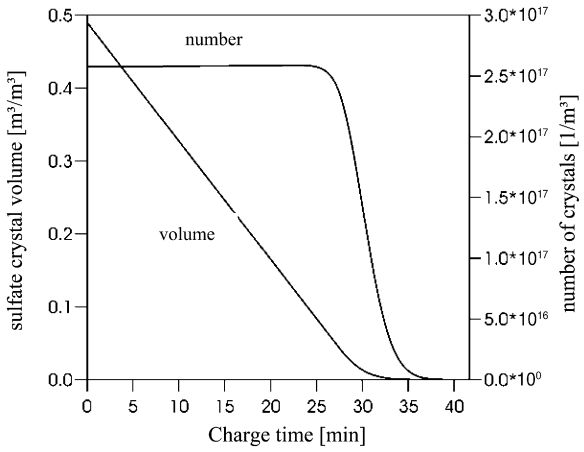

Fig. 3. Number of crystals during charging from SoC = 0.5 to 1 (simulated data from Ref. [8], charging current $5I_{10}$).

the current factor. Hence, the current factor only has to be calculated once after a full charge. The current used for the estimation of the number of crystals is the average current during the first 2% of a discharge after full charging.

If the battery undergoes incomplete full chargings, the number of crystals is reduced. This is a consequence of the fact that the size of the sulfate crystals follows a distribution function. During charging to high states-of-charge below full charging, the smaller crystals are dissolved and the larger crystals remain in the active mass. During the following discharge, the remaining crystals grow with the same consequences as mentioned above. No 'Spannungssack' is observed if the battery has not been fully charged. If the battery is fully charged, however, new crystals are formed during the initial discharge period ('Spannungssack' occurs) and the number of crystals stays nearly constant. The (simulated) variation in the number of crystals during a full charge starting from SoC = 0.5 according to Ref. [8] is given in Fig. 3. The charging current is I_1 until about 27.5 min after the start. After that, a constant voltage is used for charging and the current decreases. It can be seen that the number of crystals stays constant until about 24.5 min after the start of the charging, which corresponds to a SoC of about 0.908. Hence, charging to a lower SoC than 0.9 will not effect the number of crystals at all and should therefore not be counted as a bad charge.

Based on data from Ref. [8], the decrease in the number of crystals, z, with the number of bad recharge cycles, n, can be calculated as follows:

$$z(n) = z(0)\ \exp\left(-\frac{n}{3.6}\right) \tag{18}$$

The function is plotted in Fig. 4.

The total current factor can then be calculated as:

$$f_1(I,n) = f_1(I)\sqrt[3]{\frac{z(0)}{z(n)}} = f_1(I)\sqrt[3]{\exp\left(+\frac{n}{3.6}\right)} \tag{19}$$

The number of bad recharges, n, is increased every time the SoC reaches the state that is defined as the fully-charged state ($SoC > SoC_{limit}$). At the moment the SoC falls under that limit again, the maximum SoC since the time the SoC had reached

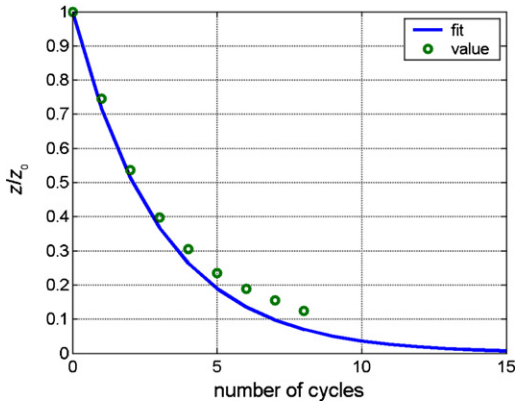

Fig. 4. Decreasing number of crystals with increasing number of incomplete recharges.

SoC_{limit} is determined and this value is used to calculate the extent to which the charge. Cycles between SoC_{limit} and 1 are not counted. If the SoC reaches 0.9999, n is reset to 0.

In order to consider the quality of the charge, the number of cycles is weighted with the maximum achieved SoC. This weighting is based on the following assumptions:

- Charging to a lower SoC than 0.9 will not affect the number of crystals at all and should therefore not be counted as a bad charge.
- Dissolving only a small number of crystals does not influence the total number of crystals very much. A significant influence on the number of crystals is detectable only if a significant number of crystals is dissolved. On the other hand, if all – or nearly all – of the crystals are dissolved during charging, there is only a little influence because during the next discharge many new crystals can be built as there are only a few crystals left.

In order to obtain a continuous function for all states-of-charge, the following function is used:

$$\Delta n = \frac{0.0025 - (SoC_{ref} - SoC_{max})^2}{0.0025} \tag{20}$$

with $SoC_{ref} = 0.95$. This function is depicted in Fig. 5.

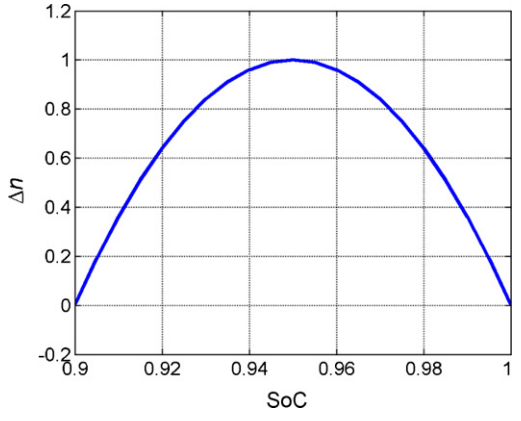

Fig. 5. Weighting factor for 'bad charging' counts.

3.4.3. Acid stratification

The degree of acid stratification is modelled by the factor $f_{\text{stratification}}$:

$$f_{\text{stratification}} = \int (f_{\text{plus}} - f_{\text{minus}})\,\mathrm{d}t, \quad f_{\text{stratification}} \geq 0 \tag{21}$$

where f_{plus} and f_{minus} represent an increase and a decrease of acid stratification, respectively.

The total impact of acid stratification on active mass degradation is modelled by the factor f_{acid}:

$$f_{\text{acid}} = 1 + f_{\text{stratification}}\sqrt{\frac{I_{\text{ref}}}{|I|}} \tag{22}$$

where I_{ref} is a reference current (typically the 10 h current). The impact of acid stratification on battery lifetime is inversely proportional to the current rate. This represents the more severe impact of small current on inhomogeneous current distribution compared with larger currents [8].

3.4.3.1. Increase of acid stratification. Acid stratification increases during cyclic operation. It is more distinct the lower the state-of-charge since the last time acid stratification is removed and the higher the discharge current. Removal of acid stratification is assumed to take place due to extensive gassing. Taking into account all the factors described above, the factor for the increase of acid stratification becomes:

$$f_{\text{plus}}(t) = c_{\text{plus}}(1 - \text{SoC}_{\text{min}}|_{t_0}^{t})\,\exp(-3 f_{\text{stratificaion}}(t))\frac{|I_{\text{dch}}(t)|}{I_{\text{ref}}} \tag{23}$$

The first factor means that if the battery experiences three full cycles without acid stratification removal by gassing with a discharge current of $I_{\text{ref}} = I_{10}$, the acid stratification factor increases by 1. This factor has been estimated by the authors from field experience and analysis of simulation results with detailed models. SoC_{min} is the lowest state-of-charge since the last full charge, which occurred at time t_0. The exponential factor is introduced to limit f_{plus} taking into account the fact that acid stratification can build up only to a certain extent.

3.4.3.2. Decrease of acid stratification. Acid stratification is removed by diffusion and by gassing. Diffusion is slow, so it is typically only noticeable during long pauses. Decrease of acid stratification by gassing only starts for voltages above $U_{\text{acid\_dec}} = 2.3$ V. Then $f_{\text{minus,gassing}}$ increases exponentially. This is based on the assumption that the mixing effect is directly proportional to the amount of gas generated in the cell. Gas generation increases exponentially with temperature and voltage. Below $U_{\text{acid\_dec}} = 2.3$ V per cell, the amount of gas generated is assumed to be too small to mix the electrolyte efficiently. The decrease of acid stratification by gassing can be calculated as follows:

$$f_{\text{minus,gassing}} = c_{\text{minus}}\sqrt{\frac{100\,\text{Ah}}{C_{\text{N}}}}\frac{I_{\text{gas,0}}(t)}{I_{\text{gas,0}}}\,\exp(c_{\text{u}}(U_{\text{cell}} - U_{\text{ref}}) + c_{\text{T}}(T - T_{\text{gas,0}})) \tag{24}$$

where U_{cell} is the cell voltage. This factor is designed to be equal to $c_{\text{minus}} = 0.1$ if $U_{\text{cell}} = U_{\text{ref}} = 2.5$ V and $T = T_{\text{gas,0}}$ for a 100 Ah battery. Acid stratification is harder to remove in large batteries than in small batteries, therefore $f_{\text{minus,gassing}}$ is weighted with the nominal battery capacity. $I_{\text{gas,0}}(t)$ is the normalized gassing current taking into account the present state of ageing of the battery, and $I_{\text{gas,0}}$ is the initial normalized gassing current.

The influence of diffusion can be calculated as follows:

$$\begin{aligned}\frac{1}{V}\frac{\partial N}{\partial t} &= D\,\nabla^2\left(\frac{N}{V}\right)\\ &= D\left(\frac{1}{V}\left(\frac{\partial^2 N}{\partial x^2} + \frac{\partial^2 N}{\partial y^2} + \frac{\partial^2 N}{\partial z^2}\right)\right.\\ &\quad \left. + 2\frac{N}{V}\left(\frac{1}{x^2} + \frac{1}{y^2} + \frac{1}{z^2}\right)\right)\end{aligned} \tag{25}$$

where N is the number of moles of HSO_4^- per volume element and V is the volume of the volume element. The effective diffusion constant, D, is in the range of $1\text{–}20 \times 10^{-9}\,\text{m}^2\,\text{s}^{-1}$ [22] and takes into account the internal geometry and the hindrance to diffusion that is imposed by the separator. If the acid gradient is assumed to be linear, the first part becomes zero. Therefore, assuming that only vertical diffusion makes a relevant contribution to the levelling of acid stratification where z is approximately the height of the electrodes, Eq. (12) becomes:

$$\frac{\partial N}{\partial t} = \frac{2DN}{z^2} \tag{26}$$

where $f_{\text{stratification}}$ is equal to zero if there is no concentration gradient and it increases with increasing concentration gradient. Therefore, it can be used as a substitute to N whereas $\partial N/\partial t$ is substituted by the change in the acid stratification ($f_{\text{minus,diffusion}}$). Assuming that the average diffusion distance is $z/2$ and that there is a temperature dependency according to the Arrhenius law, the following equation can be formulated:

$$\begin{aligned}f_{\text{minus,diffusion}} &= \frac{2D}{(z/2)^2} f_{\text{stratification}} 2^{(T-20\,^\circ\text{C})/10\,\text{K}}\\ &= \frac{8D}{z^2} f_{\text{stratification}} 2^{(T-20\,^\circ\text{C})/10\,\text{K}}\end{aligned} \tag{27}$$

As an example, this factor models removal of acid stratification by diffusion within 130 days for $D = 1 \times 10^{-9}\,\text{m}^2\,\text{s}^{-1}$ and $z = 30$ cm.

The factor for the total decrease of acid stratification is:

$$f_{\text{minus}} = f_{\text{minus,gassing}} + f_{\text{minus,diffusion}} \tag{28}$$

3.5. Time evolution of parameters affected by ageing

At the end of each simulation step, the new resistance and capacity parameters are calculated. Both the ohmic resistances for charging and discharging (cf., Eq. (1)) are increasing due to the resistance of the corrosion layer at a certain point of time:

$$\rho_{\text{c}}(t) = \rho_{\text{c}}(0) + \rho_{\text{corr}}(t), \qquad \rho_{\text{d}}(t) = \rho_{\text{d}}(0) + \rho_{\text{corr}}(t) \tag{29}$$

Table 1
Battery-dependent parameters, example for a flat-plate battery (OGi) with a flooded electrolyte that is recommended by the manufacturer for photovoltaic applications

Parameter	Description	Value	In Eq.
C_N	Nominal capacity	54 Ah (data sheet)	Various
Z_{IEC}	Number of cycles under standard conditions	600 (data sheet)	(14)
L	Float lifetime	10 years (data sheet)	(11)
U_0	Open-circuit voltage at full charge	2.1 V	(1)
g	Gradient of change in OCV with state-of-charge	0.076 V	(1)
ρ_c/ρ_d	Effective internal resistance	0.42 Ω Ah/0.699 Ω Ah	(1)
M_c/M_d	Resistance representing charge-transfer process which depends on state-of-charge	0.888/0.0464	(1)
C_c/C_d	Normalized capacity of battery	1.001/1.75	(1)
I_{ref}	Normalized reference current for current factor	−55 A	(18)
z	Height of battery	20 cm	(27)

The remaining battery capacity is the initial battery capacity minus the capacity loss by corrosion and degradation, i.e.:

$$C_{remaining}(t) = C_d(t) = C_d(0) - C_{corr}(t) - C_{deg}(t) \quad (30)$$

The parameter C_c remains unchanged, as it represents the maximum state-of-charge. Within this model, a battery is always fully charged if all the remaining active materials are converted into the charged state. Non-active materials cannot be converted and thus reduce the discharge capacity.

3.6. Set of parameters (example)

3.6.1. Parameters that depend on the battery

These are parameters that have to be measured, or taken from the data sheet, for each battery that is to be modelled. By way of example, Table 1 gives the battery-dependent parameters for a flat-plate electrode battery (OGi) with a flooded electrolyte that is recommended by the manufacturer for photovoltaic applications.

3.6.2. Parameters that could be changed

These parameters are mostly values that parameterize physical processes in the battery, which have been obtained either from expert guesses or from evaluating measured data of some batteries. It is probably possible to obtain better simulation results by varying slightly these parameters. This has to be done very carefully, however, and therefore it is recommended to leave the parameters as they are. Nevertheless, it is possible to identify more suitable parameters. The parameters that could be adapted if appropriate measured lifetime data are available are listed in Table 2.

3.6.3. Parameters that should not be changed

These parameters, which are given in Table 3, are mostly values without direct physical meaning that have been determined from fitting.

4. Simulation results

As a part of an EU project [23], several measurements with two types of battery were performed. OGi batteries (flat-plate with a flooded electrolyte, electrodes are thicker than for automotive batteries) with a capacity $C_N = 54$ Ah and OPzS batteries (flooded electrolyte, where the positive electrode is a tubular-plate and the negative is a flat-plate electrode) with $C_N = 50$ Ah were used for lifetime tests that consist of a typical

Table 2
Parameters that can be adapted if appropriate measured lifetime data are available

Parameter	Description	Value	In Eq.
$U_{corr,0}$	Corrosion voltage of fully-charged battery without current flow	1.75 V	(5)
$I_{gas,0}$	Normalized gassing current at $U_{gas,0}$ and $T_{gas,0}$	20 mA[a]	(6)
c_u	Voltage coefficient of gassing current	11 V^{-1}	(6)
c_T	Temperature coefficient of gassing current	0.06 K^{-1}	(6)
$U_{gas,0}$	Nominal voltage for gassing	2.23 V	(6)
$T_{gas,0}$, $T_{corr,0}$	Nominal temperature for gassing and corrosion	298 K	(6) and (9)
$k_{s,T}$	Temperature coefficient of corrosion speed	ln(2)/15 K^{-1}	(9)
$c_{SoC,0}$	Constant slope for SoC factor	6.614×10^{-5} h^{-1}	(15)
$c_{SoC,min}$	Impact of the minimum SoC on the SoC factor	3.307×10^{-3} h^{-1}	(15)
SoC_{limit}	Minimum state-of-charge for bad charges	0.90	
SoC_{ref}	Reference state-of-charge for bad charges	0.95	(20)
c_{plus}	Factor for increase of acid stratification	1/30	(24)
c_{minus}	Factor for decrease of acid stratification with gassing	0.1	(24)
U_{ref}	Reference voltage for decreasing acid stratification	2.5 V	(24)
U_{acid_dec}	Voltage at which gassing starts to remove acid stratification	2.3 V	
D	Diffusion constant for sulfuric acid	20×10^{-9} m^2 s^{-1}	(27)

[a] Typical value for the normalized gassing current for a new battery with antimony grid alloys. For VRLA battery typically 10 mA/100 Ah. For aged batteries the normalized gassing can increase by a factor 5 or more.

Table 3
Parameters that should not be changed

Parameter	Description	Value	In Eq.
c_Z	Exponent for calculation of capacity loss due to degradation	5	(13)
z_0 (cm^{-3})	Coefficient of number of sulfate crystals	2.961×10^{11}	(18)

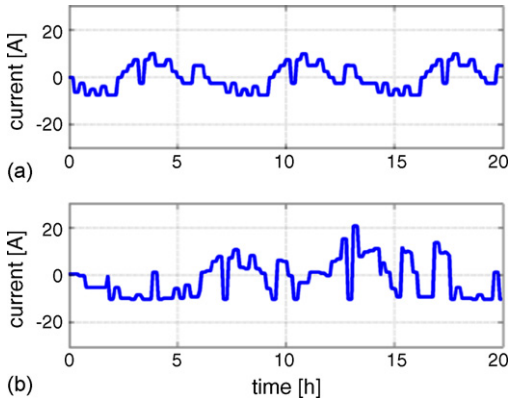

Fig. 6. (a) PV and (b) wind current profile used to verify model [23].

current profile of an autonomous power-supply system with either a wind generator or a photovoltaic generator (see Fig. 6 [23]). Capacity tests were performed regularly.

4.1. Comparison of wind and PV profiles with two types of battery

Measurements were undertaken at the CRES research centre in Greece and contain all possible combinations that were investigated in the project, namely, OGi battery with wind and PV current profile as well as OPzS battery with wind and PV current profile. The resulting data were used to parameterize the model in order to find one parameter set that fits both profiles with both batteries. It is noted, however, that some parameters, e.g., those of the Shepherd equation (Eq. (1)) for the voltage estimation, are battery specific and therefore differ for the two types of batteries. A comparison of measurement and simulation for an OGi battery with the PV profile is shown in Fig. 7. In curve (a), the measured (red stars) and simulated (blue line) capacity are compared and the SoC is depicted. The voltage is shown in curve (b) and the input current and the current that is used for the calculation of the current factor are given in curve (c). Some factors that influence degradation are presented in Fig. 8. In curve (a) the weighted and unweighted number of cycles Z_W and Z_N are compared, in curve (b) the SoC and current weighting factors and number of bad charges are given and in curve (c) the progression of the acid stratification weighting factors f_{Acid}, f_{minus} and f_{plus} is shown.

A comparison of the measured and the simulated capacity for the remaining combinations of battery type (OGi and OPzS) and wind or PV profile is given in Fig. 9. The four simulations are in good agreement with the measured values and are all done with the same parameter set. The only difference is the current

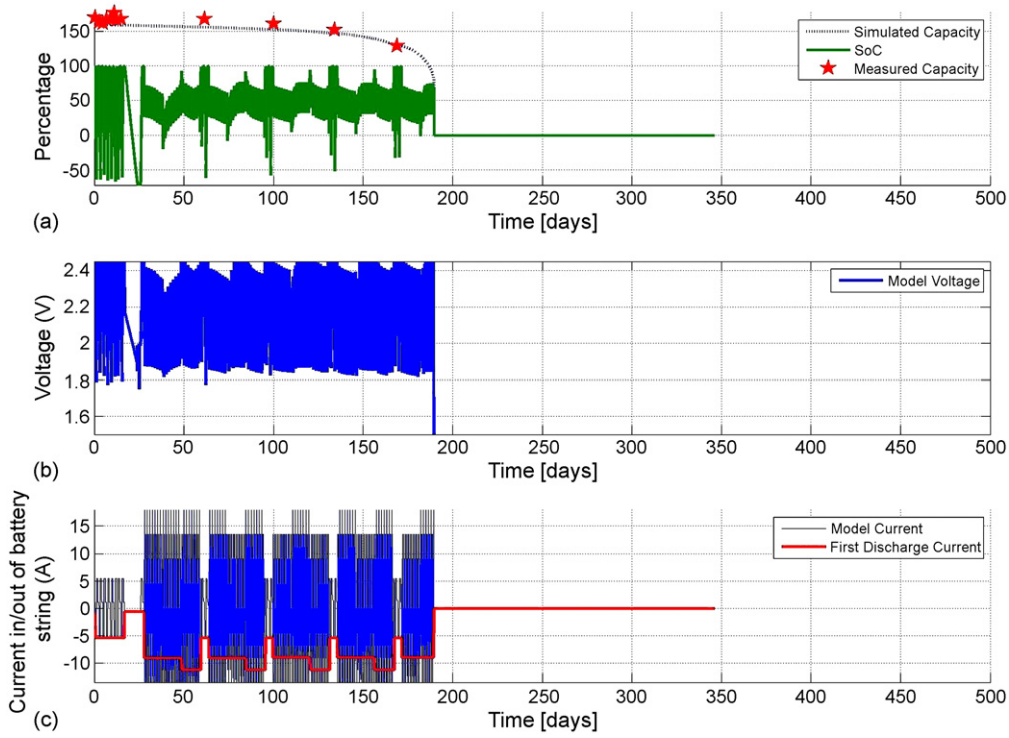

Fig. 7. Measurement and simulation for OGi battery, PV profile at CRES: (a) remaining capacity, SoC and measured capacity (red stars), (b) voltage and (c) current. (For interpretation of the references to colour in this figure legend, the reader is referred to the web version of the article.)

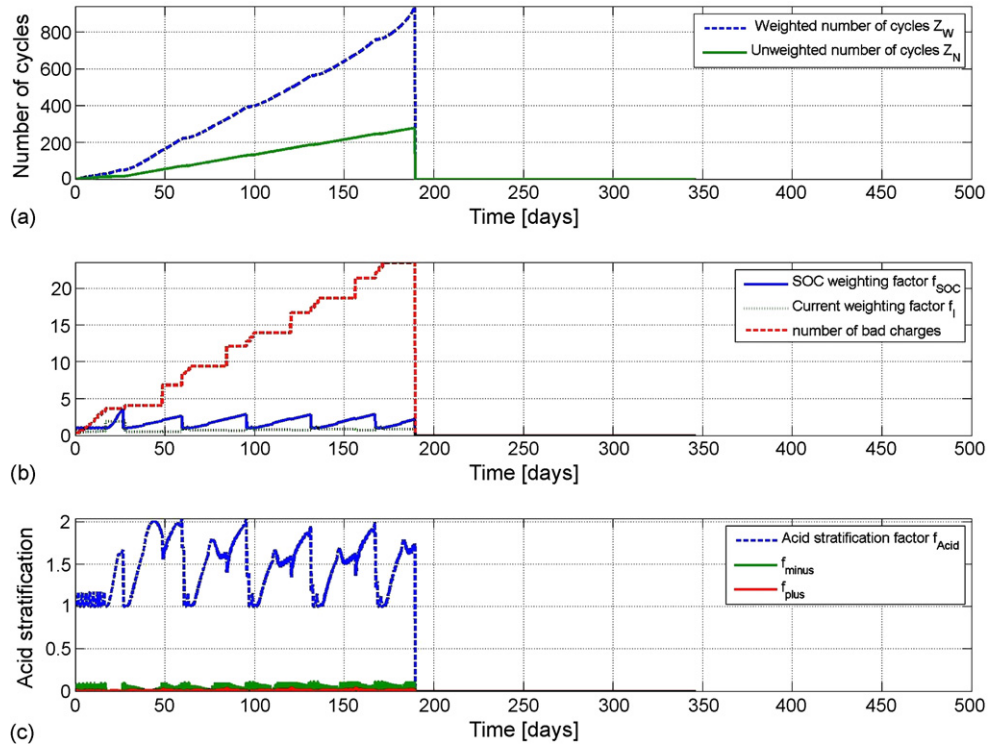

Fig. 8. OGi battery, PV profile at CRES: (a) weighted and unweighted number of cycles Z_W and Z_N, (b) SoC and current weighting factors and number of bad charges, and (c) acid stratification weighting factors f_{Acid}, f_{minus} and f_{plus}. (For interpretation of the references to colour in this figure legend, the reader is referred to the web version of the article.)

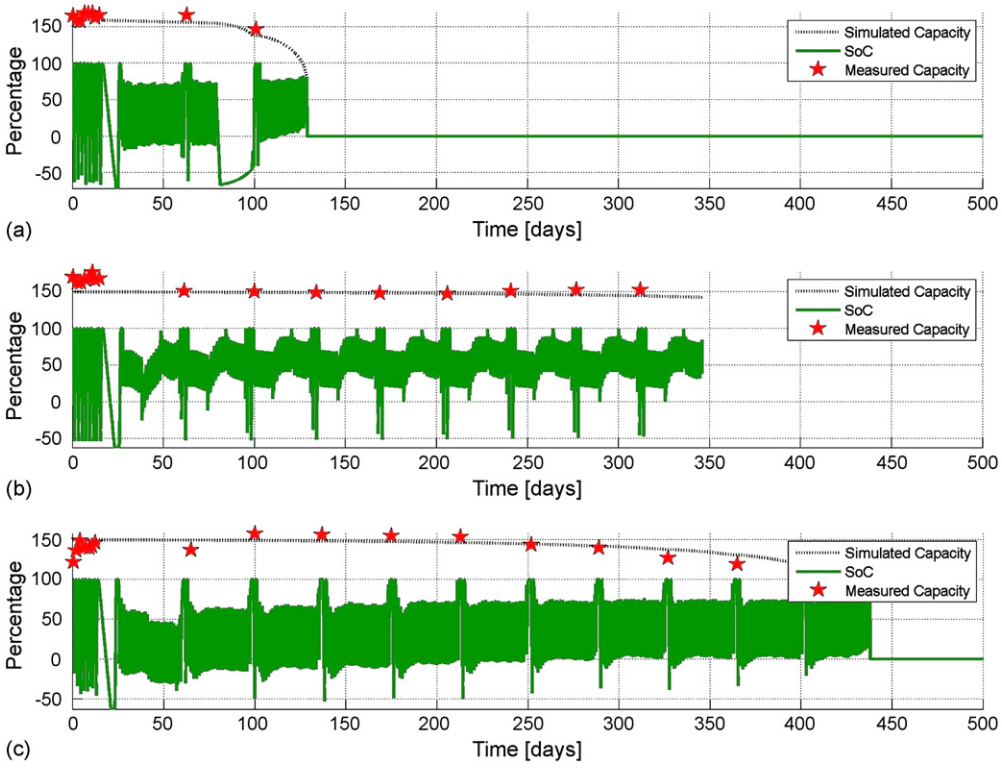

Fig. 9. Comparison of measurement and simulation for (a) OGi battery with wind profile and OPzS battery with (b) PV (profile) and (c) wind profile. (For interpretation of the references to colour in this figure legend, the reader is referred to the web version of the article.)

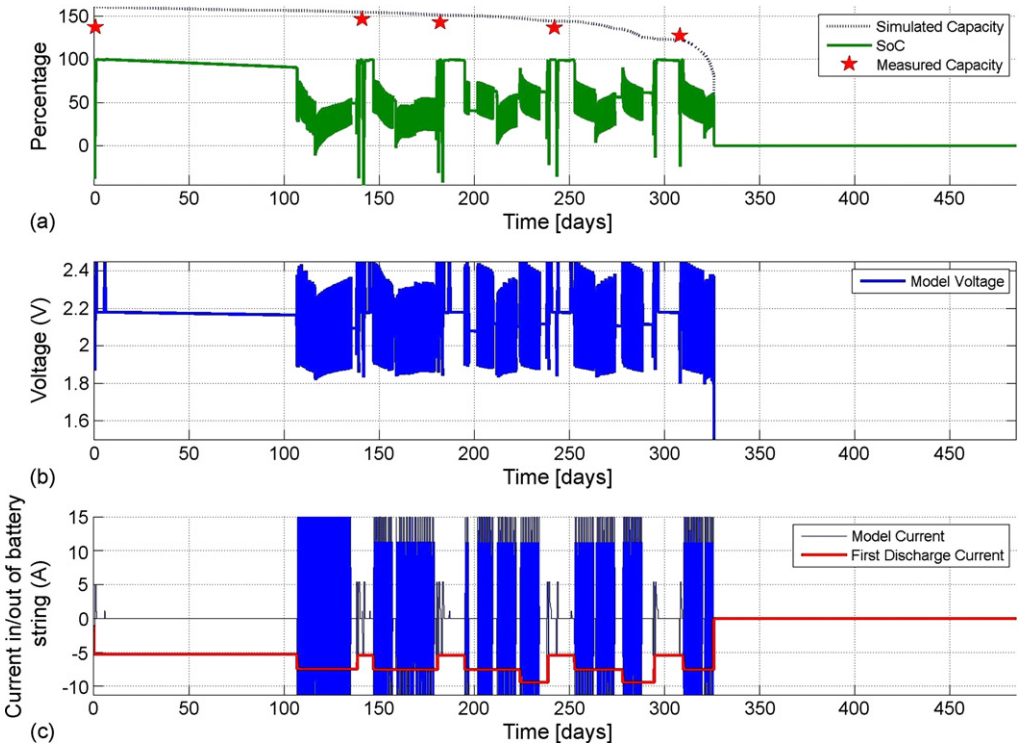

Fig. 10. Measurement and simulation for OGi battery, PV profile at ISPRA: (a) remaining capacity, SoC and measured capacity (red stars), (b) voltage and (c) current. (For interpretation of the references to colour in this figure legend, the reader is referred to the web version of the article.)

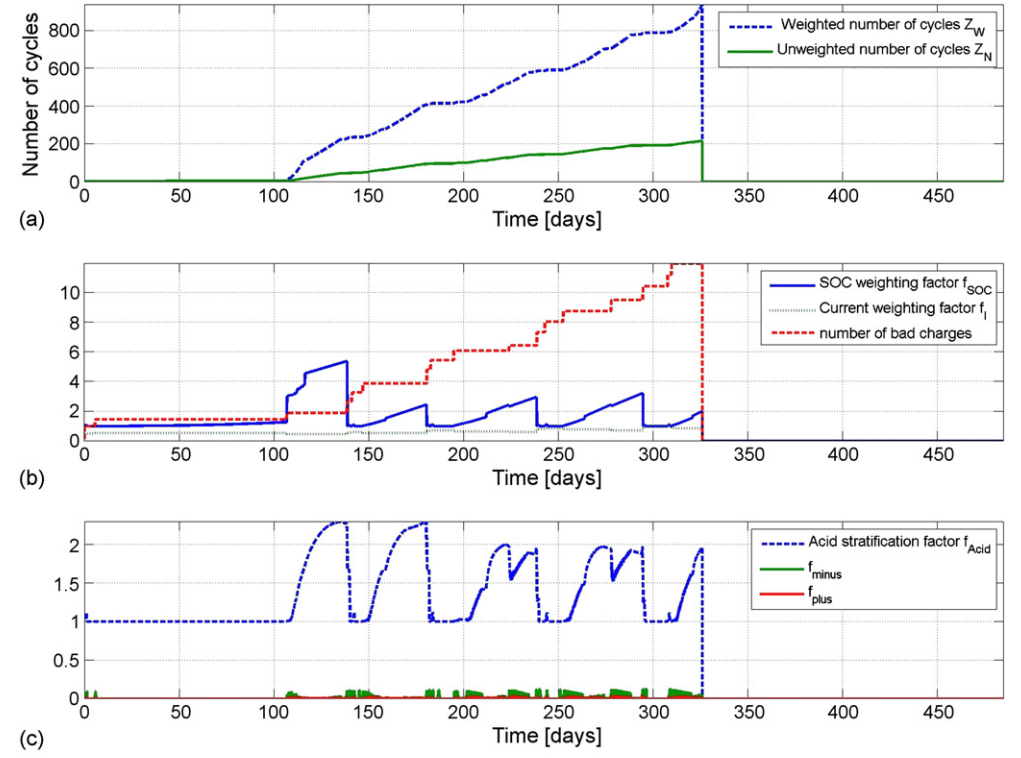

Fig. 11. OGi battery, PV profile at ISPRA: (a) weighted and unweighted number of cycles Z_W and Z_N; (b) SoC and current weighting factors and number of bad charges, and (c) acid stratification weighting factors f_{Acid}, f_{minus} and f_{plus}. (For interpretation of the references to colour in this figure legend, the reader is referred to the web version of the article.)

Table 4
Lifetime data from data sheet of two batteries, IEC cycles according to IEC 60896-1

	Float lifetime in years	IEC cycles
OPzS	14	1400
OGi	10	600

profile and some parameters that are specific for the type of battery. The lifetime data for the two batteries that were used in the simulation are presented in Table 4.

4.2. Simulation including pauses

Other measurements during the benchmarking project were conducted at ISPRA with an OGi battery and a PV current profile. The measurements contain a pause of about 3 months. Although the model was not originally meant to represent such a long pause, which typically does not occur in PV or wind applications, the model is also able to simulate pauses. Comparisons of measurement and simulation are given in Figs. 10 and 11. During the pause, the current and acid stratification weighting factor stay constant, while the SoC weighting factor increases slightly because of the self-discharge that can also be seen in the SoC curve in Fig. 10(a).

5. Conclusion

A battery lifetime prediction model, which can be used in system design tools and which is optimized for high computing speed, has been developed. It allows analysis of the expected lifetime under different operating conditions and system designs. Even though the model is easy to use, the internal complexity is high and takes into account several aspects such as acid stratification, charging strategies and impact of current rates. The model has been parameterized to work with two different types of flooded lead-acid batteries and then further improved to allow simulation of PV and wind current profiles as well as pauses. The adaptation to different battery types is achieved by using the data sheet information on float lifetime and nominal capacity lifetime. It is necessary to accept that the model cannot be better than the quality of this data sheet information. The model is a valuable tool for system design and optimization as well as for system simulations like in [24].

References

[1] J.J. Lander, J. Electrochem. Soc. 98 (1951) 213–219.
[2] J.J. Lander, J. Electrochem. Soc. 98 (1951) 220–224.
[3] J.J. Lander, J. Electrochem. Soc. 103 (1956) 1–8.
[4] P. Ruetschi, B.D. Cahan, J. Electrochem. Soc. 105 (1958) 369–377.
[5] P. Ruetschi, R.T. Angstadt, J. Electrochem. Soc. 111 (1964) 1323.
[6] P. Ruetschi, J. Electrochem. Soc. 120 (1973) 331.
[7] H. Bode, Lead-acid Batteries, John Wiley & Sons, 1977.
[8] D.U. Sauer, Dissertation, University of Ulm, Germany, 2003.
[9] D.U. Sauer, J. Power Sources 64 (1997) 181–187.
[10] F. Mattera, D. Desmettre, J.L. Martin, Ph. Malbranche, J. Power Sources 113 (2003) 400–407.
[11] A. Jossen, J. Garche, D.U. Sauer, Solar Energy 76 (2004) 759–769.
[12] D.U. Sauer, J. Garche, J. Power Sources 95 (2001) 130–134.
[13] W. Kappus, Electrochim. Acta 28 (1983) 1529–1537.
[14] C.P. de Oliveira, M.C. Lopes, J. Power Sources 138 (2004) 294–300.
[15] A. Delaille, M. Perrin, F. Huet, L. Hernout, J. Power Sources 158 (2006) 1019–1028.
[16] C.M. Shepherd, J. Electrochem. Soc. 112 (1965) 657–664.
[17] J. Schumacher-Gröhn, PhD thesis, University of Oldenburg, 1991.
[18] D. Linzen, E. Karden, D.U. Sauer, J. Schiffer, E. Surewaard, Proceedings of the 21st Electrical Vehicle Symposium—EVS21, Monaco, 2–6 April, 2005.
[19] A. Stöcklein, Diploma thesis, University of Oldenburg, 1993.
[20] D. Berndt, Maintenance-free Batteries: Lead-Acid, Nickel/Cadmium, Nickel/Metal Hydride: A Handbook of Battery Technology, 3rd ed., Research Studies Press Ltd., Taunton, Somerset, England, 2003.
[21] H.G. Puls, Diploma thesis, University of Freiburg and Fraunhofer ISE, Germany, 1997.
[22] A. Jossen, Säureschichtung in Bleibatterien, http://www.basytec.de/Literatur/saeure.pdf.
[23] H. Bindner, T. Cronin, P. Lundsager, J.F. Manwell, U. Abdulwahid, I. Baring-Gould, Lifetime Modelling, Report on WP 4.1 of EU Benchmarking Research Project (ENK6-CT-2001-80576), 2005. http://www.benchmarking.eu.org/Publications/Publications.htm, last visit 4 August 2006.
[24] H. Bindner, T. Cronin, P. Lundsager, A. Andersson, D.U. Sauer, J. Schiffer, Proceedings of the 3rd European PV Hybrid and Minigrid Conference, Aix-en-Provence, 11–12 May, 2006.